Nose Temperature and Anticorrelation between Recrystallization Kinetics and Molecular Relaxation Dynamics in Amorphous Morniflumate at High Pressure

*Michela Romanini,[†] Sergio Rodriguez, Sofia Valenti, María Barrio, Josep Lluis Tamarit, Roberto Macovez**

Grup de Caracterització de Materials, Departament de Física and Barcelona Research Center in Multiscale Science and Engineering, Universitat Politècnica de Catalunya, EEBE, Campus Diagonal-Besòs, Av. Eduard Maristany 10-14, E-08019 Barcelona, Catalonia, Spain.

* Corresponding author: roberto.macovez@upc.edu

ABSTRACT

We probe the dielectric response of the supercooled liquid phase of Morniflumate, an active principle with anti-inflammatory and antipyretic properties, studying in particular the pressure and temperature dependence of the relaxation dynamics, glass transition temperature T_g, and recrystallization kinetics. T_g increases by roughly 20 K every 100 MPa at low applied pressure, where the ratio T_g/T_m has a constant value of ~ 0.8 (T_m = melting point). Liquid Morniflumate displays two dielectric relaxations: the structural α relaxation associated with the collective reorientational motions which become arrested at T_g, and a secondary relaxation likely corresponding to an intramolecular dynamics. The relaxation times of both processes scale approximately with the inverse reduced temperature T_g/T. Near room temperature and under an applied pressure of 50 MPa, supercooled Morniflumate recrystallizes in a characteristic time of few hours, with an Avrami exponent of 1.15. Under these conditions, the recrystallization rate is a nonmonotonic function of temperature, displaying a maximum around 298 K, which can be taken to be the optimum crystal growth temperature T_{nose}. The β relaxation becomes kinetically frozen at ambient temperature under an applied hydrostatic pressure higher than 320 MPa, suggesting that the Morniflumate glass should be kinetically stable under these conditions.

KEYWORDS: glassy drug stability, dielectric spectroscopy, secondary relaxation, recrystallization kinetics, optimum crystal growth temperature.

1. Introduction

In recent years many active pharmaceutical ingredients (APIs) with poor aqueous solubility have reached the drug development stage by means of formulation in the amorphous solid or supercooled liquid state.[1-4] Below the melting temperature, the amorphous form of an API (both supercooled liquid and glass) has lower density and higher free energy than the crystalline phase. This entails on one hand that the amorphous API has a better dissolution profile in the biological medium and thus a higher bioavailability,[5] but on the other hand, that such phase is thermodynamically unstable against recrystallization into the poorly soluble crystal phase.[6] In this context, it is of interest to study the amorphous form of APIs and the recrystallization kinetics, and to determine the metastability conditions of this non-equilibrium form and whether strategies can be devised to maintain it for longer storage times.[7]

It has been suggested by several authors that the recrystallization rate and onset times, and therefore indirectly the kinetic stability of the amorphous phase, are directly correlated with the characteristic times of molecular relaxation processes in the amorphous phase, both above the glass transition temperature,[8,9] where the dynamics is dominated by the cooperative structural (α) relaxation which vitrifies at T_g, and below such temperature, where only secondary relaxations take place.[10,11] These secondary relaxations can correspond to local, intramolecular motions involving the rotation of a polar subpart of a molecule, or else be so called Johari-Goldstein (JG) relaxations. The JG relaxation is a molecular dynamics process of glass forming materials that involves the motion of the constituent molecules as a whole, but that contrary to the α relaxation is active also in the glass state below T_g.[12,13] It is found in many instances that, as a rule of thumb, the amorphous state of an API can be maintained for a commercially significant time if it is stored well below the glass transition, following the so-called "T_g – 50 K" rule.[14-16] The relatively high

kinetic stability of the amorphous phase under these conditions is related to a slow nucleation and growth kinetics of the crystal phase; nucleation is generally avoided deep in the glass state, unless other external stimuli are applied, inducing phenomena such as strain-induced fracture[17] or electric-field dependent polymorphism.[18] Recent studies indicate that the "T_g – 50 K" rule should be reformulated in terms of the freeze temperature of secondary relaxations, that is, long-term kinetic stability of the glass state against recrystallization can be obtained at a storage temperature below the temperature at which the secondary relaxations freeze out.[11,19]

It has been suggested that obtaining the amorphous phase under high pressure conditions may improve its kinetic stability, based on the fact that T_g increases with increasing pressure. However, this conjecture has not been tested in detail; the effect of applying a pressure on a supercooled liquid is in some cases opposite, with an increased tendency towards nucleation of the crystalline phase, possibly due to pressure-induced shock accelerating nucleation.[20,21] The effect of the increased density on the crystallization kinetics is instead different for different compounds.[22] In general, the relaxation dynamics and recrystallization kinetics are much less studied under an applied hydrostatic pressure than at atmospheric pressure.

The application of pressure allows studying for example the possible existence, for the relaxation times of the studied dynamic processes, of scaling relations such as the so-called density-dependent "thermodynamic scaling",[23-27] whose range of applicability is debated,[28,29] or the master-curve scaling as a function of the inverse reduced temperature T_g/T. A common scaling of the secondary relaxation time and of the structural relaxation time is considered to be a distinctive feature of the JG relaxation,[30] which is generally not shared by local relaxations corresponding to the reorientational motions of polar subgroups of a molecule.[31]

In this contribution, we employ broadband dielectric spectroscopy to study the dependence on pressure and temperature of the relaxation dynamics of a glass-forming anti-inflammatory drug, Morniflumate, as well as its recrystallization kinetics at high pressure. The glass transition temperature displays a very large increase by almost 90 K when the pressure is increased from ambient conditions to 520 MPa. The dielectric loss spectra are characterized by the presence of a structured, multicomponent main loss feature. By application of pressure, we are able to distinguish two separate spectral contributions, and to assign them respectively to the structural relaxation (α) associated with the collective diffusional motions which become frozen at the glass transition, and to a secondary (β) relaxation likely of intramolecular nature. While the β relaxation has approximately constant activation energy and volume, the α relaxation time displays sub-Arrhenius temperature dependence and an effective activation volume that increases with increasing pressure. Despite the fact that both α and β relaxation times follow a common scaling as function of the inverse reduced temperature T_g/T, the secondary relaxation lacks other characteristic traits of JG relaxations.

By monitoring the recrystallization kinetics at a pressure of 50 MPa near ambient temperature, we find that crystallization of supercooled Morniflumate follows the Avrami law with exponent n = 1.15 which suggests a strongly anisotropic, one-dimensional growth of the crystallites with sporadic nucleation of new domains. Optical microscopy investigation of samples recrystallized under these conditions indeed shows a dendritic-like growth. The recrystallization time is found to be a nonmonotonic function of temperature, with an optimum crystallization temperature near room temperature (298 K) at 50 MPa. In particular, the recrystallization time has the opposite temperature dependence than the primary and secondary relaxation times above 300 K, invalidating the idea that the mutual correlation between these quantities reported in several recent

studies[8,9,32-34] can be a general feature of amorphous APIs. At the same time, we provide a rationalization for the previous observations of such mutual correlation by means of ambient pressure dielectric spectroscopy.

Finally, assuming that well below T_g the correlation between secondary relaxation time and recrystallization time is recovered and that the relation recently proposed by Kissi *et al.*[11] is valid, we estimate that the recrystallization of amorphous Morniflumate should be effectively quenched, at ambient temperature, by the application of a hydrostatic pressure of 320 MPa.

2. Experimental Methods

High-Pressure Differential Thermal Analysis (HP-DTA)

A home-made high-pressure differential thermal analyzer (HP-DTA), similar to the apparatus reported in Ref. 35 and working in the pressure range 0.1-300 MPa, was used to determine the glass transition temperatures and melting points of unweighed Morniflumate specimens in cylindrical tin pans, sealed so as to avoid the presence of air bubbles. The set-up was in thermal contact with a bath containing the cryogenic liquid Kryo 51 by Lauda, which allowed varying the sample temperature between 223 and 393 K. HP-DTA scans were acquired upon heating at a rate of 2 K min^{-1}.

Ambient-Pressure and High-Pressure Dielectric Spectroscopy

For dielectric measurements, Morniflumate was placed inside home-made stainless steel parallel-plate capacitors designed for measuring liquid samples in the radiofrequency range, with the plates kept separated by needle-like cylindrical silica spacers of 50 μm diameter. For temperature control, the capacitor was loaded in either a nitrogen-gas cryostat operating between 120 and 500 K at ambient pressure, or a pressure set-up in thermal contact with a bath of the Kryo

51 liquid, which allowed sample temperature control between 223 and 393 K. In the pressure set-up, the maximum pressure available was 520 MPa.

The sample was initially melted to reach the supercooled liquid state, and dielectric spectra were then acquired between 10^{-1} and $5 \cdot 10^{6}$ Hz at fixed values of pressure and temperature, with a typical temperature stability of ±0.3 K and a pressure stability better than 0.5 MPa, respectively. Four series of spectra were acquired while keeping the temperature constant and varying the pressure (isothermal series), and three more series while keeping a fixed pressure and varying the temperature (isobaric series).

A Novocontrol Alpha analyzer was employed for dielectric characterization, connected to the capacitor plates via electrical contacts, and dielectric data were analyzed with the dedicated WinFit software by the same producer. The isothermal dielectric spectra are complex functions of frequency, which can be displayed as real permittivity spectra (the dielectric function, ε'(*f*)) and imaginary permittivity spectra (the loss spectrum, ε"(*f*)). The ε"(*f*) spectra were fitted as the sum of two relaxation processes α and β, each modeled as the imaginary part of the phenomenological Cole-Cole function (ε_{CC}), and a background representing the dc conductivity contribution:

(1) $\varepsilon(f) = -i\left(\frac{\sigma_0}{\varepsilon_0 2\pi f}\right)^n + \varepsilon_{CC,\alpha}(f) + \varepsilon_{CC,\beta}(f)$

The analytical expression of ε_{CC} is:[36,37]

(2) $\varepsilon_{CC}(f) = \varepsilon_\infty + \frac{\Delta\varepsilon}{1+(i2\pi f\tau)^c}$

Here, $\Delta\varepsilon = \varepsilon_s - \varepsilon_\infty$ is the dielectric strength (equal to the step variation of the real part of the permittivity ε'), and ε_∞ and ε_s are the high-frequency and low-frequency (static) limits of ε'(*f*), respectively. τ is the characteristic time of each relaxation process, corresponding to the maximum dielectric loss, and the Cole-Cole exponent *c*, which lies in the range from 0 to 1, is related to the width of each relaxation feature in the loss spectrum. The fit functions used to model the relaxation

processes were of the more general Havriliak-Nagami type, whose spectral line shape is asymmetric and depends on a second exponent, but the free fits gave a better agreement with the experimental data when such exponent was equal to one, corresponding to the Cole-Cole case. The origin of the two relaxation processes will be discussed in Section 3.

Optical microscopy

Micrographs of the Morniflumate samples after recrystallization were acquired with an Olympus BX51optical microscope with an objective with 20× magnification.

3. Results and Discussion

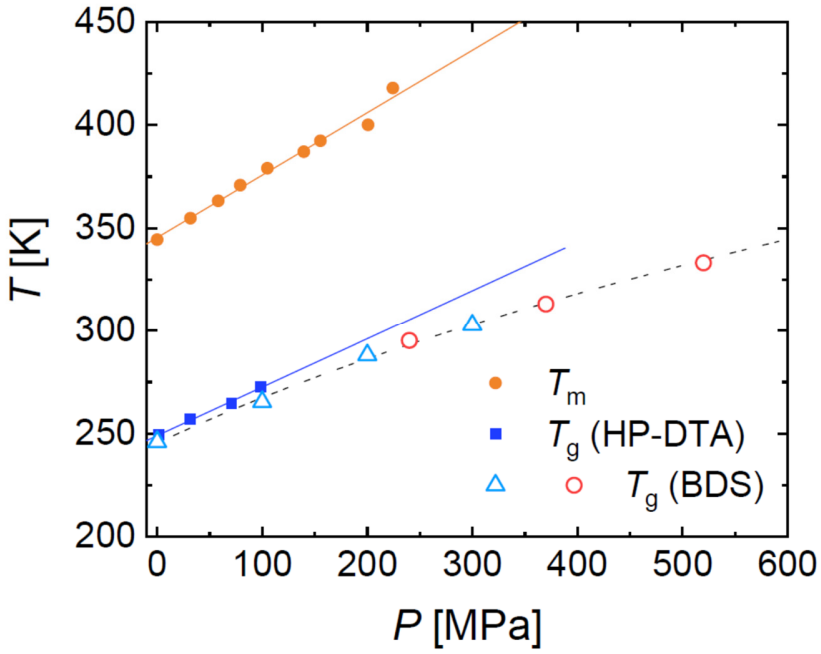

Figure 1. Filled markers: T_m and T_g of Morniflumate obtained by HP-DTA, as a function of the applied hydrostatic pressure. Continuous lines are linear fits of equations T_m [K] = 0.30 P [MPa] + 345.4 and T_g [K] = 0.23 P[Mpa] + 249.0, respectively. T_m data are taken from Ref. 38. Open markers: (T_g,P_g) pairs for Morniflumate as extracted from both isothermal (red circles) and isobaric (blue triangles) BDS measurements. Dashed line: fit with Eq. (5).

Figure 1 shows the values of the melting point (T_m) and glass transition temperature (T_g) determined in isobaric HP-DTA scans on the polycrystalline Morniflumate powder and supercooled Morniflumate, respectively. The T_m values were taken from a previous work by some of us.[38] The experimental critical temperatures for the glass-supercooled liquid transition and for the melting of the crystal phase are observed to vary roughly linearly with applied pressure. Linear fits are obtained with slopes $(dT/dP)_g = 0.235$ K/MPa and $(dT/dP)_m = 0.291$ K/MPa, respectively. The ratio of the linear coefficients is $0.235/0.291 \approx 0.808$, so that, at least for low applied pressures, the relation $T_g/T_m \sim 0.8$ holds (for many glass formers this ratio is approximately close to 2/3). It should be noted that both critical temperatures vary significantly with the applied pressure; in particular, at low applied pressure T_g increases by roughly 20 K every 100 MPa. Open markers represent (T_g,P_g) pairs obtained by dielectric spectroscopy, to be discussed later on.

Dielectric spectroscopy experiments were carried out on supercooled liquid Morniflumate in order to observe directly the effect of an applied pressure on the molecular relaxation dynamics. Figure 2 displays typical dielectric loss spectra as a function of frequency, acquired either during an isobaric experiment at 100 MPa while changing the temperature in steps of 2 K (a), or during an isothermal series at 313 K while increasing the pressure in a stepwise fashion (b). Each spectrum is characterized by a low-frequency background increasing toward lower frequencies, which corresponds to the dc conductivity contribution to the dielectric loss, and a prominent loss feature with asymmetric shape. Close-up investigation of the loss feature shows that it actually consists of two symmetric components, one responsible for the local ε" maximum, and the other visible as a shoulder on the high-frequency flank of the latter. Indeed, a fit of all spectra with Eq. (1) shows that a single Cole-Cole (or even Havriliak-Negami) function is not enough to account for the observed spectra, and that instead two (Cole-Cole) components are necessary, which we label as

α and β, respectively. The two relaxation components, the conductivity background, and the overall fit are shown in Figure 2 for selected spectra. The rest of the spectra acquired in our study (not shown) similarly displayed two relaxation components.

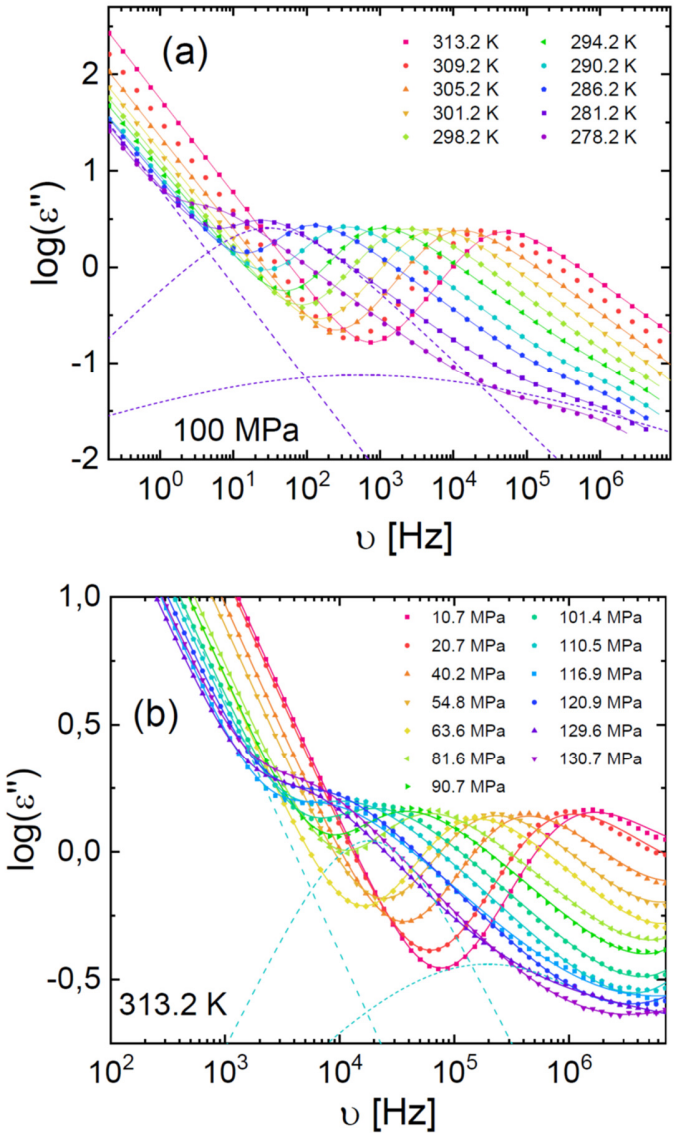

Figure 2. Selected dielectric loss spectra of Morniflumate at different (*P*,*T*) conditions (markers), and their fits with the imaginary part of Eq. (1) (continuous lines). All spectra were fitted with two spectral components. (a) Series of isobaric spectra at different temperatures as indicated, at the fixed pressure of 100 MPa. Dashed lines are fit components of the spectrum at 281.2 K. (b) Series

of isothermal spectra at different pressures as indicated, at 313.2 K. Dashed lines are fit components of the spectrum at 110.5 MPa.

The fit of the loss spectra with Eq. (1) yields the relaxation times of both relaxation processes. The resulting relaxation maps are shown in Figure 3 in two separate panels, namely as a function of the inverse temperature in the isothermal series (the so-called Arrhenius plot, panel (a)), and as a function of pressure for the isothermal series (b). Of the two processes, the faster and less intense β relaxation, appearing as a high-frequency shoulder in the loss spectrum, has a characteristic logarithmic relaxation time that varies almost linearly with 1/*T* and *P*, respectively. Instead, the logarithm of the relaxation time of the slower and more intense process (labeled as α and responsible for the local maximum of ε") displays a nonlinear dependence on these variables. As shown below, the α relaxation feature is the structural relaxation of supercooled liquid Morniflumate, which justifies the label. In the Arrhenius plot (Figure 3(a)), it is also seen that the relaxation times of the α and β processes tend have a similar dependence on temperature at sufficiently high *T*.

The temperature dependence of the relaxation time of the α process was modelled with the Vogel-Fulcher-Tammann equation, which is typical of cooperative structural processes in glass-forming liquids and whose analytical expression is:[39]

(3) $\tau_\alpha(T) = \tau_\infty exp\left(D\frac{T_{VF}}{T-T_{VF}}\right)$.

Here the prefactor τ_∞ represents the high-temperature limit value of the relaxation time, and the so-called "strength parameter" *D* and the Vogel-Fulcher temperature T_{VF} are phenomenological constants that describe the deviation of the temperature dependence of the relaxation time from a simply activated behaviour. The pressure dependence of the same relaxation time was modeled with an analogous function of *P*, namely:[40]

(4) $\tau_\alpha(P) = \tau_0 exp\left(D_P \frac{P}{P_{VF}-P}\right)$,

where τ_0 is the value of the relaxation time at the same temperature at atmospheric pressure (0.1 MPa), P_{VF} is a "Vogel-Fulcher pressure", and D_P is the equivalent strength parameter.

On the other hand, the faster (β) relaxation time had as mentioned a simply-activated Arrhenius temperature dependence $\tau_\beta(T) = \tau_\infty exp\left(\frac{E_a}{RT}\right)$, where is R the gas constant and E_a is the molar activation energy, and a linear pressure dependence $\tau_\beta(P) = \tau_0 exp\left(\frac{PV_a}{RT}\right)$, being V_a the molar activation volume. The fit parameters for both α and β relaxations are reported in Table 1.

Isobars	0.1 MPa	100 MPa	200 MPa	300 MPa
Log(τ_∞/[s])	–12.6	–9.9	–10.6	–12.6
T_{VF} (K)	207	236	250	249
D	6.4	3.4	4.4	7.4
T_g (K)	246.1±0.8	265.4±1.9	288±2	302.9±2.2
fragility (m)	91±1	108±6	96±4	81±3
E_a (β-relax) (kJ/mol)	140.5±0.4	150±2	152±3	197±2

Isotherms	292.2 K	313.2 K	333.2 K
Log(τ_0/[s])	–6.0	–7.1	–8.0
P_{VF} (MPa)	978	1002	992
D_P	52	38	22
P_g (MPa)	256±33	357±31	513±12
fragility (m)	78±21	77±18	98±16
$10^4 \cdot V_a$ (β-relax) (m^3/mol)	2.3±0.1	1.53±0.03	1.21±0.02

Table 1. Fit Parameters and Fragility Index of the α Relaxation and Activation Energy or Volume of the β Relaxation, for Isobaric (Top Rows) and Isothermal (Bottom Rows) Series.

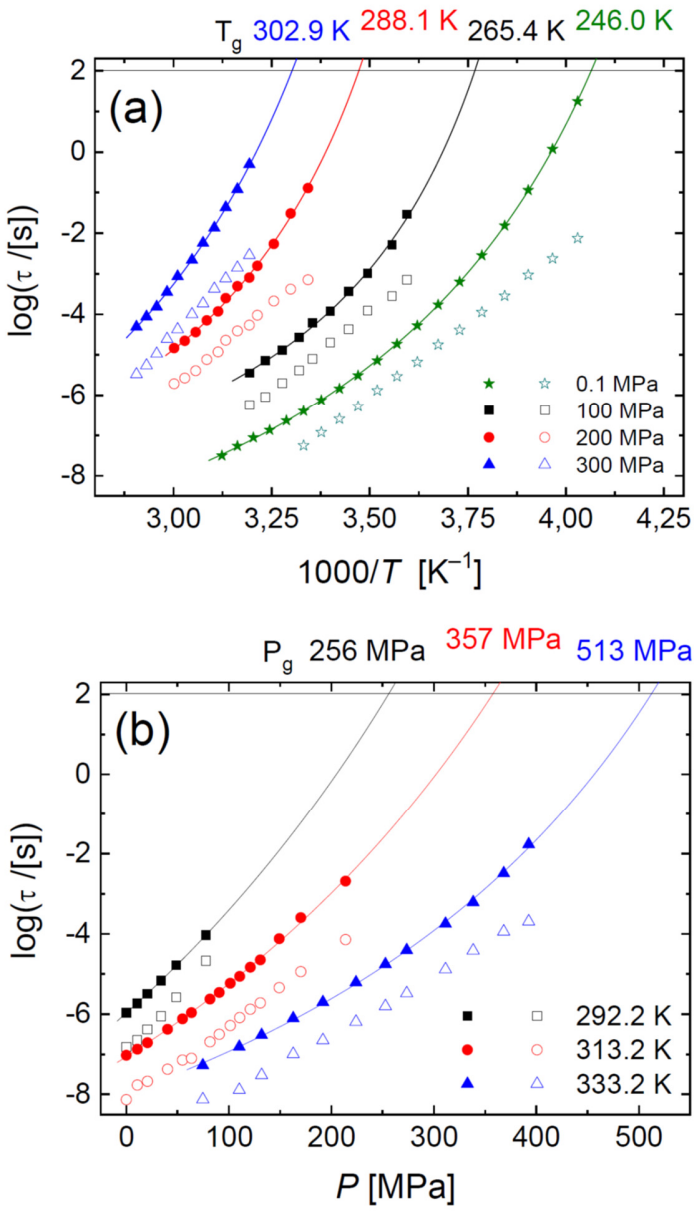

Figure 3. Relaxation maps of the structural (α, filled markers) and secondary (β, open markers) dynamic processes observed in Morniflumate in the isothermal and isobaric series. (a) Relaxation times as a function of inverse absolute temperature (Arrhenius plot), for four different isobaric series. Continuous lines are fits with Eq. (3), and the glass transition temperatures are indicated. (b) Relaxation times as a function of pressure, for three different isothermal series as indicated. Continuous lines are fits with Eq. (4), and the glass transition pressures are indicated.

Extrapolation of the exponential fit functions Eq.s (3) and (4) to the value τ_α = 100 s (that is, Log(τ_α) = 2) yields the values of the thermodynamic variables at the vitrification (freeze) temperature of the α relaxation process. These can be compared with (T_g,P_g) pairs for the glass transition obtained in HP-DTA measurements, as shown in Figure 1. The agreement between the T_g values obtained by both techniques (Figure 1) shows that the relaxation process labelled as α is indeed the cooperative structural relaxation of the Morniflumate glass former. It should be noted that, while HP-DTA measurements are conducted in a smaller pressure interval, in which the dependence of T_g on pressure appears to be linear, in a larger pressure range the same dependence is found to be sublinear. In particular, the relation between T_g and P_g is found to be well described by the empirical Andersson and Andersson equation, given by:[41]

(5) $T_g = k_1 \left(1 + \frac{k_2}{k_3} \cdot P_g\right)^{\frac{1}{k_2}}$,

Where k_1, k_2 and k_3 are material constants. The fit is displayed with a dashed line in Figure 1. The best-fit values of the parameters were k_1 = 245.3±1.5 K, k_2 = 2.9±0.5, and k_3 = 1020±90 MPa, respectively.

The relaxation times of the β relaxation can similarly be extrapolated to a value of 100 s, assuming a constant linear dependence on P and 1/T; the corresponding (T,P) values represent the thermodynamic conditions at which the secondary relaxation is effectively "frozen", and the glass state of Morniflumate should, according to a recent study, acquire sufficient kinetic stability to prevent transformation of the API into the thermodynamically stable crystal phase.[11] In particular, at ambient temperature the extrapolated "freeze pressure" of the secondary relaxation of Morniflumate is approximately 320 MPa.

It is interesting to plot all obtained relaxation times in a single plot as a function of the inverse reduced temperature T_g/T (the so-called Angell plot). This is displayed in Figure 4(a). It may be

observed that both the structural (α) and secondary (β) relaxation times of different measurements are very roughly superposed in the graph, and that the slope of the β relaxation in the Angell plot has similar values for all isobaric and isothermal series. The scaling of both α and β relaxation times with the reduced temperature is nontrivial (for example, no such scaling is observed when using the reduced pressure P/P_g). On the other hand, however, the τ_α and τ_β relaxation times do not tend to converge at the same value at high temperatures; it seems instead that the two dynamics remain separated by one decade in time in the high-T region of the plot. This is in contrast with the expectations for a Johari-Goldstein (JG) relaxation.[13,30] Another characteristic feature of JG relaxations is that, since the spectral line shape of the α relaxation is almost independent on thermodynamic variables, the value of τ_β should have virtually the same value for all (P,T) pairs with the same τ_α value; in other words, the line shape of isochronal spectra with the same structural relaxation time should be independent on T and P.[30] Figure 4(b) shows several isochronal spectra corresponding to approximately $\tau_\alpha = 5.8 \cdot 10^{-5}$ s, and it is seen that they do not all obey this invariance. We therefore conclude that the secondary β relaxation is likely a local relaxation involving the relative motions of subparts or side groups of the Morniflumate molecule.

From the curvature of the Arrhenius (Figure 3(a)) or Angell (Figure 4(a)) plots, the so-called isobaric kinetic fragility index m can be extracted, which is a measure of the degree of deviation from the simply-activated Arrhenius behaviour. The kinetic fragility is defined[42,43] as the slope to the Angell plot at $T_g/T = 1$, namely $m = \left.\frac{d(\mathrm{Log}\tau_\alpha)}{d(T_g/T)}\right|_{T=T_g}$. Using the chain rule of derivation, this steepness index can be generalized[44] to describe isothermal measurements as $m = \frac{V_a(P_g)}{R\ln(10)}\left(\frac{dT_g}{dP}\right)^{-1}$, where $V_a(P_g)$ is the extrapolated apparent activation volume of an isotherm at P_g (obtained from Eq. (4) with the corresponding fitting parameters), and dT_g/dP is the slope of the (T_g,P_g) curve

(Anderson-Anderson plot, Figure 1) at the temperature of the isotherm. The so-obtained fragility values are listed in Table 1. It is seen that Morniflumate is a relatively fragile glass former, with fragility index varying roughly between 80 and 100 depending on the applied pressure.

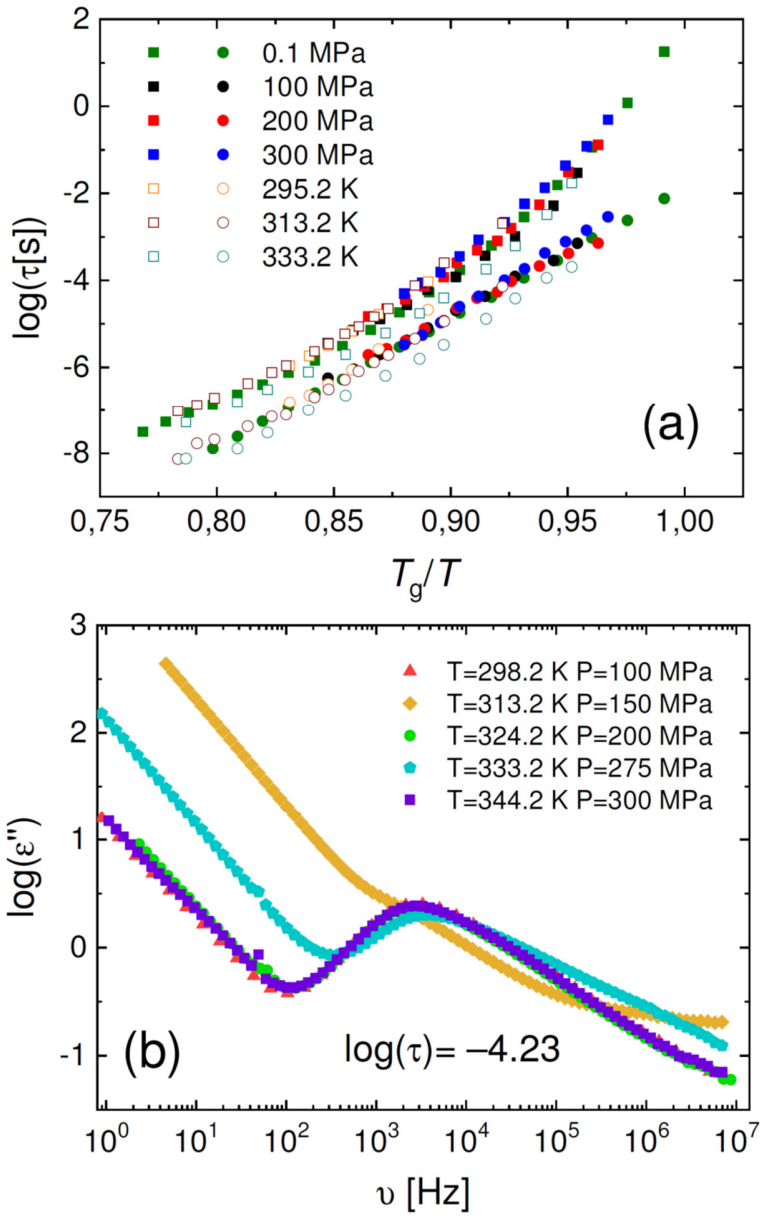

Figure 4. (a) Angell plot of the structural and secondary relaxation times of Morniflumate. Filled and open markers are data obtained from isobaric and isothermal series, respectively. (b)

Isochronal master plot of three spectra displaying approximately the same structural relaxation time ($\tau_\alpha = 5.8 \cdot 10^{-5}$ s), acquired at the indicated (T,P) conditions.

In order to determine the impact of pressure on the kinetics of recrystallization, we employed our dielectric spectroscopy setup to monitor isothermal crystallization of supercooled liquid Morniflumate near room temperature under an applied pressure of P = 50 MPa, at five different temperatures. To reach the desired state, we first melted the sample and then cooled it down to the desired temperature, and then increased the pressure from ambient pressure to 50 MPa while keeping the temperature constant (in other words, we moved towards P_g at ambient temperature with the sample in the supercooled liquid state in thermal contact with the bath at fixed temperature). The onset time of recrystallization of Morniflumate under these conditions was unpredictable: in several occasions, the sample did not show any sign of recrystallization over a period of more than one day, in another, the recrystallization started a few minutes after reaching the final desired conditions; in some cases, we induced crystallization by suddenly reducing the applied hydrostatic pressure. Visual inspection of the samples after recrystallization (see also below) showed that the nucleation was likely to occur at the interface between the sample and the electrode; in other words, nucleation was heterogeneous rather than homogeneous. As a consequence, the so-called induction time (also termed nucleation time) could not be unambiguously determined. It would appear that the "intrinsic" induction time at fixed (T,P) conditions is relatively long (more than one day), but that mechanical vibrations and especially density fluctuations induced by minimal pressure variations are sufficient to trigger nucleation of the crystal phase, as reported in other systems.[21]

We carried out a study of the crystallization kinetics by acquiring dielectric spectra at fixed (T,P) conditions and monitoring the dielectric strength of the structural relaxation process. The latter is

equal to the step-like decrease in the real permittivity visible at the characteristic frequency of the α relaxation. The series of real and imaginary permittivity spectra acquired at different times during recrystallization of Morniflumate at T = 293 K and P = 50 MPa are shown in Figure 5(a,b). The effect of recrystallization was visible as a decrease over time of the intensity of the loss feature or equivalently of the static permittivity value ε_s, the latter taken to be equal to the value of $\varepsilon'(f)$ at a frequency slightly lower than that of the α peak, at which the low-frequency plateau value of ε' is attained (at lower frequency, $\varepsilon'(f)$ increased due to polarization effects associated with mobile charge carriers). It can be observed that the relaxation frequency increases slightly during recrystallization. Such a shift was observed in most measurements, and is possibly due to the reduction in the effective internal pressure of the cell as Morniflumate crystallizes into the higher-density crystal phase or to a confinement effect on the amorphous regions.

The evolution of ε_s with the time elapsed from the start of the measurements is displayed in panel (c) of Figure 5. The onset time t_o of the recrystallization process was determined as the intersection of the horizontal line representing the constant value of ε_s in supercooled liquid Morniflumate, and the slope of the tangent to the data during recrystallization (see inset to Figure 5(c)).

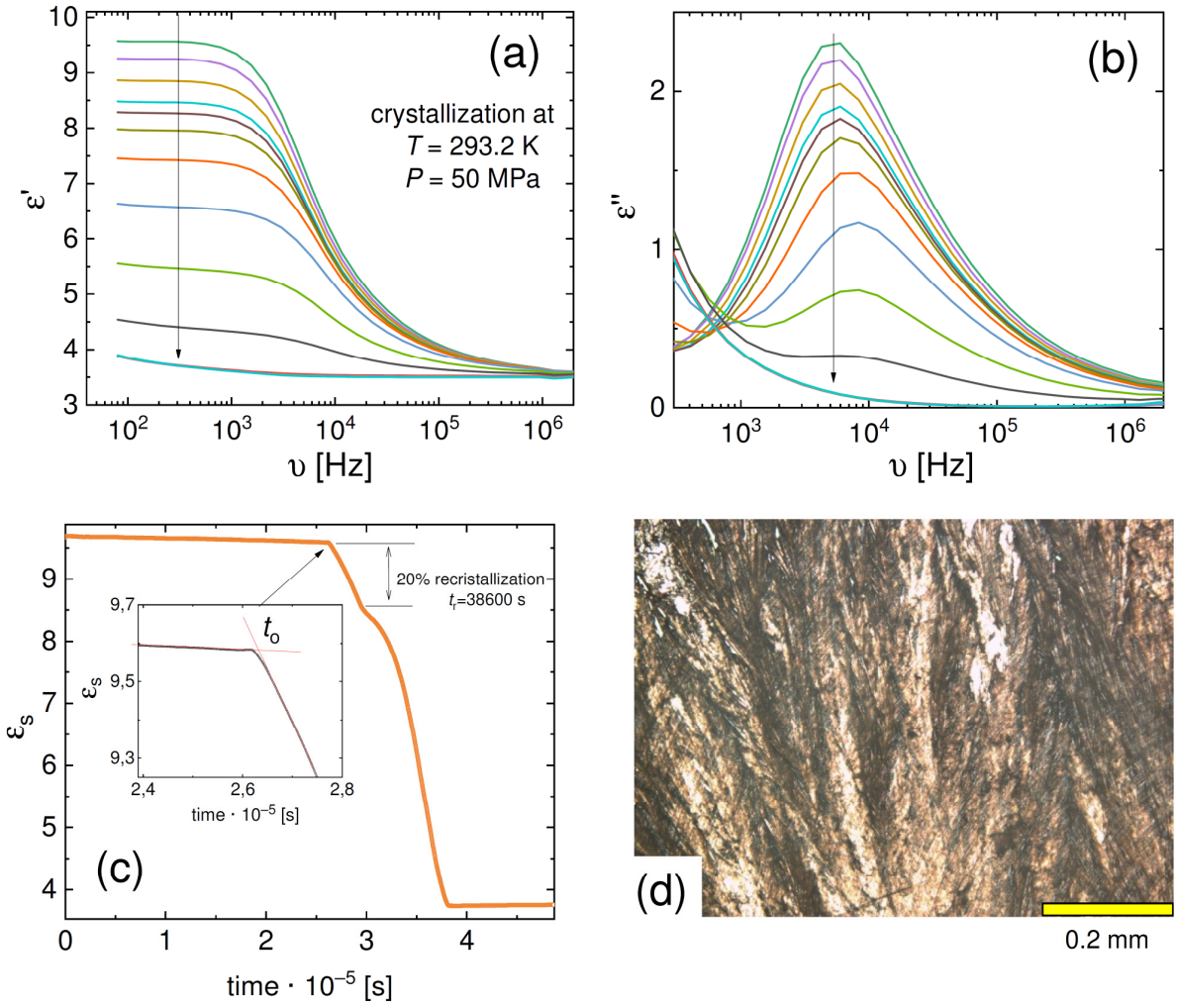

Figure 5. (a,b) Real and imaginary permittivity spectra of a supercooled Morniflumate sample during recrystallization at P = 50 MPa and T = 293 K, as a function of time elapsed since the start of the measurement. (c) Static permittivity ε_s (taken as the value of $\varepsilon'(f)$ at the frequency of 206 Hz). The determinations of the 20% recrystallization time t_r and of the onset time t_o are displayed in the main panel and in the inset, respectively (see the text for details). (d) Optical micrograph of the sample taken after full recrystallization.

In order to analyze the crystallization kinetics, we define as customary[45] a renormalized static permittivity as:

(6) $\varepsilon_n(t) = \frac{\varepsilon_s(t)-\varepsilon_s(\mathrm{SL})}{\varepsilon_s(\mathrm{C})-\varepsilon_s(\mathrm{SL})}$

Here $\varepsilon_s(\mathrm{SL})$ and $\varepsilon_s(\mathrm{C})$ are the static permittivity of the supercooled liquid and the crystal phase, as measured before the onset of nucleation of the crystal phase and at the end of the crystal growth, respectively, while $\varepsilon_s(t)$ is the static permittivity of the partially crystallized, mixed-phase sample as a function of the time elapsed from the start of the measurements. The overall global kinetics of crystallization is often described with the help of the Avrami law[46,47] which combines together the effects of both nucleation of the crystal phase and the subsequent growth of the crystalline nuclei. When the recrystallization process follows the Avrami law, the renormalized static permittivity varies in time as:[48]

(7) $\varepsilon_n(t) = 1 - \exp(-Z(t - t_o)^n)$,

where n is the Avrami exponent and Z is a constant, from which a crystallization rate with units of s^{-1} can be obtained[49] as $k = Z^{1/n}$. Eq. (7) predicts that the quantity $\ln(-\ln(1 - \varepsilon_n))$ should vary linearly with the logarithm of elapsed time since the recrystallization onset, $t - t_o$. This is indeed observed in the so-called "Avrami plot", displayed in Figure 6(a). The values of the obtained fit parameters (n, k) are listed in Table 2. While a certain variability is observed in k, as expected, the value of the Avrami exponent was always close to $n = 1.15$ for all cases.

The fact that the value of the Avrami exponent is close to unity suggests a strongly anisotropic growth of the crystalline nuclei following sporadic nucleation,[9,50,51] at least under an applied hydrostatic pressure of 50 MPa. Such anisotropic growth is confirmed by inspection of the recrystallized samples under the optical microscope (Figure 5(d)), where it is observed that the growth occurs in a dendritic fashion in the disk-like Morniflumate sample, with evidence of

nucleation sites at the edge of the disk, at the boundary with the external electrode. The latter observation implies that nucleation is mainly heterogeneous in character.

T [K]	P [MPa]	n (±0.01)	$k \cdot 10^{-5}$ [s^{-1}]	$t_r \cdot 10^{-3}$ [s]	$1/k_{n=1.15} \cdot 10^{-5}$ [s]
283.2	50	1.12	58±3	150	78±3
293.2	50	1.15	9.0±0.3	55.4	9.0±0.3
295.2	50	1.14	16.5±0.2	9.44	1.12±0.01
303.2	50	1.15	1.43±0.05	10.2	1.39±0.04
314.2	50	1.18	1.05±0.03	58.2	13.4±0.3
314.2	100	1.15	21.5±0.7	67.1	21.1±0.7
314.2	150	1.15	5.40±0.06	37.7	5.51±0.06

Table 2. Recrystallization Times and Avrami Parameters for Recrystallization of Morniflumate under Different (T,P) Conditions.

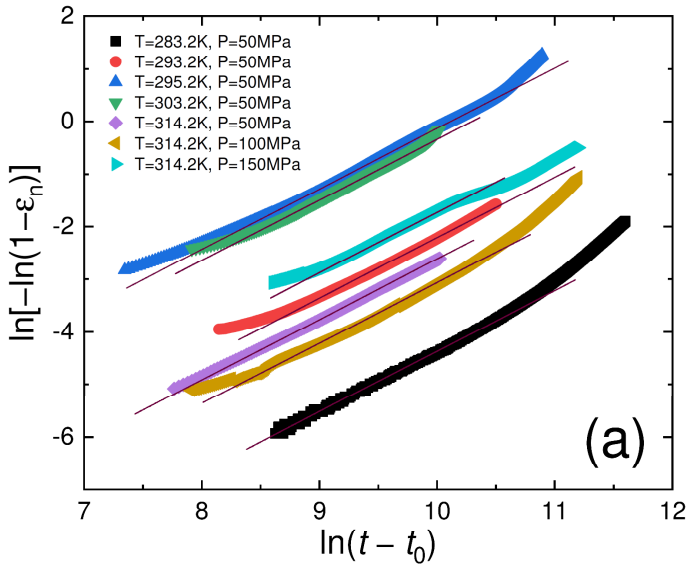
T=283.2K, P=50MPa
T=293.2K, P=50MPa
T=295.2K, P=50MPa
T=303.2K, P=50MPa
T=314.2K, P=50MPa
T=314.2K, P=100MPa
T=314.2K, P=150MPa
ln[−ln(1−εn)]
ln(t − t0)
(a)

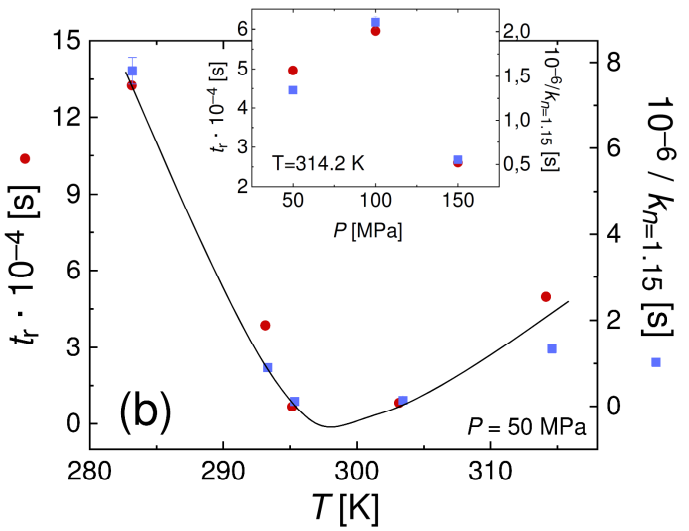
tr · 10−4 [s]
10−6 / kn=1.15 [s]
T [K]
P = 50 MPa
(b)
T=314.2 K
P [MPa]

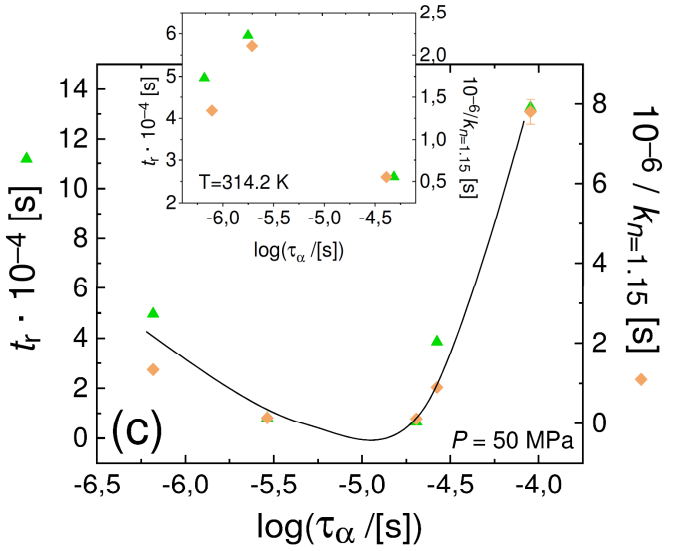
tr · 10−4 [s]
10−6 / kn=1.15 [s]
log(τα /[s])
P = 50 MPa
(c)
T=314.2 K

Figure 6. (a) Avrami plot of all recrystallization data. Markers are experimental points and continuous lines are fits with the Avrami Eq. (7). (b,c) Plot of the 20% recrystallization time t_r and of the inverse recrystallization rate $1/k_{n=1.15}$ (see the text for details) at 50 MPa as function of temperature (b) and as function of the logarithm of the structural relaxation time τ_α at the corresponding temperature (c). Continuous lines are guides to the eye. Insets: plot of t_r and $1/k_{n=1.15}$ at the fixed temperature of 312 K, as function of pressure (b) and as function of $\log(\tau_\alpha)$ at the same T, P conditions (c).

Following previous studies,[8,9,32-34,51] we define a characteristic recrystallization time t_r as the time required for a certain fraction of the supercooled liquid sample to transform to the crystalline phase (measured from the onset of crystallization), which we take here to be 20%. The values of t_r are listed in Table 2. The sporadic character of the nucleation of the crystal phase is confirmed by the fact that in many instances the onset time was significantly longer than the crystallization time, so that we can conclude that the intrinsic induction time is longer than the growth time ($t_{induction} > t_r$) for Morniflumate under the studied conditions. The values of t_r obtained at 50 MPa are plotted as a function of temperature in Figure 6(b), where it is seen that the recrystallization time is a nonmonotonic function of temperature, displaying a minimum at a temperature close to room temperature (298 K). We have also calculated a characteristic recrystallization time from the Avrami parameters, by refitting the data assuming the same value of n for all crystallizations, namely n = 1.15, and determining the corresponding inverse crystallization rate, $1/k_{n=1.15}$. The obtained values are listed in Table 2 and plotted in Figure 6(b), where it is seen that they follow exactly the same trend as t_r.

This minimum in the temperature dependence of the crystallization time is a commonly observed feature of glass formers, both organic and inorganic:[52,53] in all these systems there exists an

optimum temperature for the growth of the crystalline phase from the supercooled liquid, known as "nose temperature" from the characteristic shape of the time-temperature-transformation curve.[52,54]. The existence of the nose temperature is a consequence of two competing effects: although the thermodynamic driving force for recrystallization (difference between the free energy of the liquid and crystal states) increases as T is lowered below the melting point T_m, the molecular mobility decreases; the competition results in an optimum temperature at which recrystallization is fastest. Our results imply that the optimum crystal growth temperature T_{nose} of Morniflumate is approximately room temperature (298 K) at the pressure of 50 MPa. An increase of T above such value (at the same pressure) actually results in a slower recrystallization rate, as observed experimentally in Figure 6(b). The inset to Figure 6(b) shows the variation of t_r with pressure at the fixed temperature of 314 K. t_r has a maximum value for P = 100 MPa, while it has a lower value at 50 or 150 MPa. Applying a pressure leads to three different effects: a change in thermodynamic driving force, a change in the molecular dynamics, and a change in density; a detailed recrystallization study as a function both of T and P under isochronal conditions would be required to disentangle the three effects, which is beyond the scope of our work.

In the Figure 6(c) we plot the characteristic recrystallization time t_r and inverse recrystallization rate $1/k_{n=1.15}$ at 50 MPa at different temperatures (same data as in panel (b)), as function of the structural relaxation time τ_α at the same (T,P) conditions used in our recrystallization study. . It may be observed that the crystallization time is a nonmonotonic function of τ_α, which is a consequence of the fact that, at constant pressure, the structural relaxation time is a monotonic function of T (Figure 3(a)) while t_r and $k_{n=1.15}$ are not (Figure 6(b)). In particular, above the nose temperature the two times are "anticorrelated": τ_α decreases as the crystallization time increases. Hence the power-law correlation between t_r and τ_α observed for other pharmaceutical compounds

at ambient pressure[8,9,32-34,51] cannot be a general feature of amorphous pharmaceuticals in a large temperature window; indeed, it may be observed *a priori* only below the optimum crystal growth temperature T_{nose}. Since T_{nose} normally lies between the glass transition temperature T_g (below which the structural relaxation is kinetically frozen) and the melting point T_m, between T_{nose} and T_m the two times are necessarily anticorrelated. On the other hand, a power law correlation between t_r and τ_α can exist between T_g and T_{nose}, since at low enough temperature the recrystallization rate is fundamentally limited by the molecular mobility, that is, by the diffusion of molecules which enables formation and growth of crystal nuclei. The fact that this correlation has been often reported in dielectric spectroscopy studies is likely a consequence of the fact that the available frequency range of this technique (up to 1 or 10 MHz) is particularly suited to study dynamics close to the glass transition temperature, rather than those close to the melting point, where the structural relaxation frequency is normally above 1 or 10 GHz.

The practical implication of our findings for amorphous pharmaceuticals are two. On one hand, the fact that the possible (sublinear) correlation between the recrystallization rate and the structural relaxation time can at best hold only in a limited temperature interval (namely, between T_g and T_{nose}) indicates that one should look at secondary relaxations, rather than at the structural one, to search possible indicators of the stability of amorphous pharmaceuticals. This is of course obvious below T_g, where the structural relaxation is dynamically frozen. On the other hand, the fact that depressurization of over-pressurized liquid Morniflumate often lead in our experiments to the onset of recrystallization, indicates that pressurization may not be a viable means to stabilize amorphous pharmaceuticals: besides being scarcely applicable on an industrial scale, depressurization after storage may induce the very transformation (recrystallization) which the applied pressure might avoid during storage.

Conclusions

We have employed dielectric spectroscopy to study the pressure and temperature dependence of the relaxation dynamics and recrystallization kinetics of a glass-forming API with anti-inflammatory and antipyretic properties, Morniflumate. The dielectric spectra are characterized by the presence of two loss features, the structural α relaxation and a secondary β relaxation, respectively. Both relaxation times have a steep dependence with pressure. In particular, while the β relaxation has fixed activation volume, the α relaxation time displays an effective activation volume that increases with increasing pressure. At low applied pressure, the pressure-dependent glass transition temperature $T_g(P)$ increases by 20 K every 100 MPa. In the whole pressure and temperature range probed, both α and β relaxation times are observed to scale roughly with the temperature rescaled to the pressure-dependent glass transition temperature. Since the β relaxation can be kinetically frozen at ambient temperature by applying a pressure of approximately 320 MPa, we predict that Morniflumate should be in a kinetically stable glassy state at this pressure. The recrystallization kinetics at a pressure of 50 MPa follows the Avrami law with exponent n = 1.15, consistent with the dendritic-like growth that we observed in our freshly recrystallized samples by optical microscopy. The recrystallization time is a nonmonotonic function both of temperature and of the structural relaxation time: the optimum crystallization temperature of Morniflumate is found to be between 295 and 300 K under an applied pressure of 50 MPa.

AUTHOR INFORMATION

Corresponding Author

* Author to whom correspondence should be addressed. Electronic mail:roberto.macovez@upc.edu.

PresentAddress

† Departament d'Estructura i Constituents de la Matèria, Facultat de Física, Universitat de Barcelona, Av. Diagonal 647, E-08028 Barcelona, Catalonia, Spain.

Author Contributions

The manuscript was written through contributions of all authors. All authors have given approval to the final version of the manuscript.

ACKNOWLEDGMENT

This work has been partially supported by the Spanish Ministry of Economy and Competitiveness MINECO through project FIS2017-82625-P, and by the Generalitat de Catalunya under project 2017SGR-42.

REFERENCES

1. Shah, N., Sandhu, H., Choi, D.S., Chokshi, H., Malick, A. W. *Amorphous Solid Dispersions: Theory and Practice* (Springer, New York, 2014).

2. Yin, S., Franchini, M., Chen, J., Hsieh, A., Jen, S., Lee, T., Hussain, M., Smith, R. Bioavailability Enhancement of a COX-2 Inhibitor, BMS-347070, from a Nanocrystalline Dispersion Prepared by Spray-Drying. *J. Pharm. Sci.* 2005, 94, 1598–1607.

3. Wu, T., Yu, L. Surface Crystallization of Indomethacin Below Tg. *Pharm. Res.* 2006, 23, 2350–2355.

4. Qian, F., Tao, J., Desikan, S., Hussain, M., Smith, R. Mechanistic Investigation of Pluronic® Based Nano-crystalline Drug-polymer Solid Dispersions. *Pharm. Res.* 2007, 24,1551–1560.

5. Gupta, P., Chawla, G., Bansal, A. Physical Stability and Solubility Advantage from Amorphous Celecoxib: the Role of Thermodynamic Quantities and Molecular Mobility. *Mol. Pharmaceutics* 2004, 1, 406−413.

6. Bhardwaj, S., Arora, K., Kwong, E., Templeton, A., Clas, S., Suryanarayanan, R. Correlation between Molecular Mobility and Physical Stability of Amorphous Itraconazole. *Mol. Pharmaceutics* 2013, 10, 694−700.

7. Capen, R., Christopher, D., Forenzo, P., Ireland, C., Liu, O., Lyapustina, S., O'Neill, J., Patterson, N., Quinlan, M., Sandell, D., Schwenke, J., Stroup, W., Tougas, T. On the shelf life of pharmaceutical products. *AAPS Pharm. Sci. Tech.* 2012, 13, 911–918.

8. Mehta, M.; Ragoonanan, V.; McKenna, G. B.; Suryanarayanan, R. Correlation between Molecular Mobility and Physical Stability in Pharmaceutical Glasses. *Mol. Pharmaceutics* 2016,13, 1267−1277.

9. Ruiz, G. N., Romanini, M., Barrio, M., Tamarit, J. Ll., Pardo, L. C., Macovez, R. Relaxation Dynamics vs Crystallization Kinetics in the Amorphous State: The Case of Stiripentol. *Mol. Pharmaceutics* 2017, 14, 3636-3643.

10. Okamoto, N., Oguni, M. Discover of Crystal Nucleation Proceeding much below the Glass Transition Temperature in a Supercooled Liquid. *Solid State Commun.* 1996, 99, 53−56.

11. Kissi, E. O., Grohganz, H., Löbmann, K., Ruggiero, M. T., Zeitler, J. A., Rades, T. Glass-Transition Temperature of the β-Relaxation as the Major Predictive Parameter for Recrystallization of Neat Amorphous Drugs. *J. Phys. Chem. B* 2018, 122, 2803.

12. Johari, G. P., Goldstein, M. Viscous Liquids and the Glass Transition. II. Secondary Relaxations in Glasses of Rigid Molecules. *J. Chem. Phys.* 1970, 53, 2372–2388.

13. Ngai, K. L., Capaccioli, S. Relation between the Activation Energy of the Johari-Goldstein β Relaxation and Tg of Glass Formers. *Phys. Rev. E* 2004, 69, 031501.

14. Yu, L. Amorphous Pharmaceutical Solids: Preparation, Characterization and Stabilization. *Adv. Drug Delivery Rev.* 2001, 48, 27−42.

15. Hancock, B. C., Zografi, G. Characteristics and Significance of the Amorphous State in Pharmaceutical Systems. *J. Pharm. Sci.* 1997, 86, 1−12.

16. Hatley, R. H. M. Glass Fragility and the Stability of Pharmaceutical Preparations-Excipient Section. *Pharm. Dev. Technol.* 1997, 2, 257−264.

17. Su, Y., Yu, L., Cai, T. Enhanced Crystal Nucleation in Glass-Forming Liquids by Tensile Fracture in the Glassy State. *Cryst. Growth Des.* 2019, 19, 291−299.

18. Adrjanowicz, K., Paluch M., Richert, R. Formation of New Polymorphs and Control of Crystallization in Molecular Glass-Formers by Electric Field. *Phys. Chem. Chem. Phys.* 2018, 20, 925–931.

19. Kolodziejczyk, K., Paluch, M., Grzybowska, K. Grzybowski, A. Wojnarowska, Z., Hawelek, L., Ziolo, J. D. Relaxation Dynamics and Crystallization Study of Sildenafil in the Liquid and Glassy States. *Mol. Pharmaceutics* 2013, 10, 2270–2282.

20. Knapik, J., Wojnarowska, Z., Grzybowska, K., Hawelek, L., Sawicki, W., Wlodarski, K., Markowski, J., Paluch M. Physical Stability of the Amorphous Anticholesterol Agent (Ezetimibe): the Role of Molecular Mobility. *Mol. Pharmaceutics* 2014, 11, 4280–4290.

21. Rams-Baron, M., Pacułt, J., Jędrzejowska, A., Knapik-Kowalczuk, J., Paluch, M. Changes in Physical Stability of Supercooled Etoricoxibafter Compression. *Mol. Pharmaceutics* 2018, 15, 3969–3978.

22. Adrjanowicz, K., Grzybowski, A., Kaminski, K., Paluch, M. Temperature and Volume Effect on the Molecular Dynamics of Supercooled Ibuprofen at Ambient and Elevated Pressure. *Mol. Pharmaceutics* 2011, 8, 1975–1979.

23. Tölle, A. Neutron Scattering Studies of the Model Glass Former Ortho-terphenyl. *Rep. Prog. Phys.* 2001, 64, 1473–1532.

24. Casalini, R., Roland, C. M. Thermodynamical Scaling of the Glass Transition Dynamics. *Phys. Rev. E* 2004, 69, 062501.

25. Dreyfus, C., Le Grand, A., Gapinski, J., Steffen, W., Patkowski, A. Scaling the α-Relaxation Time of Supercooled Fragile Organic Liquids. *Eur. Phys. J. B* 2004, 42, 309–319.

26. Roland, C. M., Hensel-Bielowka, S., Paluch, M., Casalini, R. Supercooled Dynamics of Glass-Forming Liquids and Polymersunder Hydrostatic Pressure. *Rep. Prog. Phys.* 2005, 68, 1405-1478.

27. Dyre, J. C. Hidden Scale Invariance in Condensed Matter. *J. Phys. Chem. B* 2014, 118, 10007–10024.

28. Sanz, A., Hecksher, T., Wase Hansen, H., Dyre, J. C. Niss, K., Pedersen U. R. Experimental Evidence for a State-Point-Dependent Density-Scaling Exponent of Liquid Dynamics. *Phys. Rev. Lett.* 2019, 122, 055501.

29. Romanini, M., Barrio, M., Macovez, R., Ruiz-Martin, M.D., Capaccioli, S., Tamarit, J. Ll. Thermodynamic Scaling of the Dynamics of a Strongly Hydrogen-Bonded Glass-Former. *Sci. Rep.*2017, 7, 1346.

30. Ngai, K. L., Habasaki, J., Prevosto, D., Capaccioli, S., Paluch, M. Thermodynamic Scaling of α-Relaxation Time and Viscosity Stems from the Johari-Goldstein β-Relaxation or the Primitive Relaxation of the Coupling Model. *J. Chem. Phys.* 2012, 137, 034511.

31. Kaminska, E., Kaminski, K., Paluch, M., Ngai, K. L. Primary and Secondary Relaxations in Supercooled Eugenol and Isoeugenol at Ambient and Elevated Pressures: Dependence on Chemical Microstructure. *J. Chem. Phys.* 2006, 124, 164511.

32. Johari, G., Kim, S., Shanker, R. Dielectric Relaxation and Crystallization of Ultraviscous Melt and Glassy States of Aspirin, Ibuprofen, Progesterone, and Quinidine. *J. Pharm. Sci.* 2007, 96, 1159–1175.

33. Dantuluri, A. K. R., Amin, A., Puri, V., Bansal, A. K. Role of α-Relaxation on Crystallization of Amorphous Celecoxib above Tg Probed by Dielectric Spectroscopy. *Mol. Pharmaceutics* 2011, 8, 814–822.

34. Sanz, A.; Niss, K. Coupling between Molecular Mobility and Kinetics of Crystal Growth in a Hydrogen-Bonded Liquid. *Cryst. Growth Des.* 2017, 17, 4628−4636.

35. Würflinger, A. Differential Thermal Analysis under High Pressure IV: Low-Temperature DTA of Solid-Solid and Solid-Liquid Transitions of Several Hydrocarbons up to 3 kbar. *Ber. Bunsenges. Phys. Chem.* 1975, 79, 1195–1201.

36. Cole, K.S., Cole, R.H. Dispersion and Absorption in Dielectrics - I Alternating Current Characteristics. *J. Chem. Phys.* 1941, 9, 341–352.

37. Cole, K.S., Cole, R.H. Dispersion and Absorption in Dielectrics - II Direct Current Characteristics. *J. Chem. Phys.* 1942, 10, 98–105.

38. Barrio, M., Tamarit, J. Ll., Céolin, R., Robert, B., Guéchot, C., Teulon, J.-M., Rietveld, I. B. Experimental and Topological Determination of the Pressure-Temperature Phase Diagram of Morniflumate, a Pharmaceutical Ingredient with Anti-Inflammatory Properties. *J. Chem. Thermodynamics* 2017, 112, 308-313.

39. Kremer, F., Schönhals, A. *Broad Band Dielectric Spectroscopy*. (Springer, Berlin, 2003).

40. Paluch, M., Rzoska, S. J., Habdas, P., Ziolo, J. On the Isothermal Pressure Behaviour of the Relaxation Times for Supercooled Glass-Forming Liquids. *J. Phys.: Condens. Matter* 1998, 10, 4131.

41. Andersson, S. P., Andersson, O. Relaxation Studies of Poly(propylene glycol) under High Pressure. *Macromolecules* 1998, 31, 2999–3006.

42. Angell, C. A. Spectroscopy Simulation and Scattering, and the Medium Range Order Problem in Glass. *J. Non-Cryst. Solids* 1985, 73, 1–17.

43. Böhmer, R., Ngai, K. L., Angell, C. A., Plazek, D. J. Nonexponential relaxations in strong and fragile glass formers. *J. Chem. Phys.* 1993, 99, 4201-4209.

44. Paluch, M., Gapinski, J., Patkowski, A., Fischer, E. W. Does Fragility Depend on Pressure? A Dynamic Light Scattering Study of a Fragile Glassformer. *J. Chem. Phys.* 2001, 114, 8048-8055.

45. D'Amore, A. J. M. L., Kenny, J. M., Nicolais, L., Tucci, V. Dynamic-Mechanical and Dielectric Characterization of PEEK Crystallization. *Polym. Eng. Sci.* 1990, 30, 314.

46. Avrami, M. Kinetics of Phase Change. I. General theory. *J. Chem. Phys.* 1939, 7, 1103–1112.

47. Avrami, M. Kinetics of Phase Change. II Transformation-Time Relations for Random Distribution of Nuclei. *J. Chem. Phys.* 1940, 8, 212–224.

48. Adrjanowicz, K., Kaminski, K., Wojnarowska, Z., Dulski, M., Hawelek, L., Pawlus, S., Paluch, M. Dielectric Relaxation and Crystallization Kinetics of Ibuprofen at Ambient and Elevated Pressure. *J. Phys. Chem. B* 2010, 114, 6579–6593.

49. Yousefzade, O., Valenti, S., Puiggali, J., Garmabi, H., Macovez, R. Segmental Relaxation and Partial Crystallization of Chain-Extended Poly(L-Lactic Acid) Reinforced with Carboxylated Carbon Nanotube. *J. Polym. Sci. B Polym. Phys.* 2019, 57, 222–233.

50. Tripathi, P., Romanini, M., Tamarit, J. Ll., Macovez, R. Collective Relaxation Dynamics and Crystallization Kinetics of the Amorphous Biclotymol Antiseptic. *Int. J. Pharmaceutics* 2015, 495, 420–427.

51. Valenti, S., Romanini, M., Franco, L., Puiggalí, J., Tamarit, J. Ll., Macovez, R. Tuning the Kinetic Stability of the Amorphous Phase of the Chloramphenicol Antibiotic. *Mol. Pharmaceutics* 2018, 15, 5615−5624.

52. Uhlmann, D. R. A Kinetic Treatment of Glass Formation. *J. Non-Cryst. Solids* 1972, 7, 337–348.

53. Shelby, J. E. *Introduction to Glass Science and Technology, 2nd Edition* (The Royal Society of Chemistry, Cambridge, 2005).

54. Uhlmann, D. R. Glass Formation, a Contemporary View. *J. Amer. Ceram Soc.* 1983, 66, 95–100.

For Table of Contents Use Only

TOC Graphics